Identification of PTPLAD1 as a Novel Tumor Suppressor and its Implication in Metastatic Colon Cancer Therapy

Jie Yang
Jinan University
Yangjia Li
Jinan University
Yang Hu
Jinan University
Weixia Zhang
Jinan University
Xin Yan
Jinan University
Junze Liang
Jinan University
Xiaohui Huang
Jinan University
Bin Li
Jinan University
Qing-Yu He (tqyhe@jnu.edu.cn)
Jinan University https://orcid.org/0000-0003-0503-9492

Research

Keywords: PTPLAD1, PHB/Raf/ERK/Snail signaling pathway, Colon cancer metastasis, Avobenzone, Novel targeted drug

Posted Date: October 6th, 2021

DOI: https://doi.org/10.21203/rs.3.rs-942066/v1

Abstract

Background: Colon cancer is one of the most common malignant cancers, and cancer metastasis always leads to a failure of clinical treatment. Although there have been many studies on the process of colon cancer progression, the detailed mechanism of colon cancer metastasis still remains unclear, and more effective drugs targeting colon cancer metastasis are urgently needed. This study aims to explore novel effectors involved in colon cancer metastasis and screen out potential targeted drug for colon cancer therapy.

Methods: Mass spectrometry and bioinformatics analyses are performed to present the proteomics variation between two colon cancer cell lines with different invasion abilities. Boyden chamber invasion assay (*in vitro*) and experimental metastasis assay in mice (*in vivo*) are performed to explore the role of protein tyrosine phosphatase-like A domain containing 1 (PTPLAD1) in colon cancer metastasis. Western blotting and qRT-PCR assays are performed to analyze the expression of proteins and mRNA of related signaling cascades. Co-immunoprecipitation (Co-IP) and confocal assays are conducted to examine the proteins interacted with PTPLAD1. Chromatin-immunoprecipitation (ChIP) assay is fulfilled to evaluate the relationship of PTPLAD1 expression and histone H3K9 acetylation. Enzyme-linked immuno sorbent assay (ELISA) screening system are used to screen out the small molecular inhibitor that mimics the effect of PTPLAD1 on suppressing colon cancer metastasis.

Results: Our results identify that PTPLAD1 is significantly downregulated in the highly invasive cell lines, and PTPLAD1 suppresses colon cancer metastasis by interacting with prohibitin (PHB) and prohibiting the activation of PHB/C-Raf1 (Raf)/ extracellular signal-regulated kinase (ERK)/Snail signaling pathway. Moreover, the expression of PTPLAD1 is modulated through the acetylation of histone H3K9. Besides, we identify a small molecule named avobenzone, once used to protect skin from ultraviolet damage, that can disrupt the interaction of PHB and Raf, significantly abrogate the activation of downstream signaling cascades and prohibit colon cancer metastasis.

Conclusions: Collectively, our study not only identifies PTPLAD1 as a novel tumor suppressor and clarifies its role in suppressing colon cancer metastasis, but also provides a potential targeted drug for metastatic colon cancer therapy.

Background

Colon cancer is the third most commonly diagnosed malignant cancer in men and the second most commonly diagnosed malignant cancer in women, and cancer metastasis is responsible for most colon cancer deaths [1]. Although there have been adequate advances in our understanding of the mechanism of colon cancer metastasis, efficient remedies for the prevention and treatment of metastatic colon cancer are still missing, and valuable tumor biomarkers and diagnostic targets are urgently needed [2].To further identify the mechanism that is responsible for colon cancer metastasis, we compared the proteomics variation of SW480 and SW620, two colon cancer cell lines derived from one Caucasian

patient in different pathological stages, where SW620 is more invasive than SW480 [3]. Among the differentially expressed proteins identified, protein tyrosine phosphatase-like A domain containing 1 (PTPLAD1) drew our attention.

The *PTPLAD1* gene was first identified in sodium butyrate-treated mouse fibroblasts and encodes the PTPLAD1 protein with 360 amino acids in mice and 362 amino acids in humans [4]. Protein structure analysis of PTPLAD1 in Homo sapiens shows a CS domain in the N-terminus, a PTPLA domain in the C-terminus and a linker peptide in the middle segment [4]. A previous study reported that PTPLAD1 interacts with ELOVL proteins and is involved in very long-chain fatty acid (VLCFA) synthesis [5]. Another study claimed that PTPLAD1 interacts with the small GTPase Rac and appears to be involved in Rac1 signaling and finally suppresses NF-κB activity, thus inhibiting cell proliferation and inducing differentiation [4]. Studies have demonstrated that PTPLAD1 interacts with hepatitis C virus (HCV) NS5A and regulates viral replication during HCV infection [6, 7]. A study also validated that the expression of PTPLAD1 could affect the interaction between insulin receptors, tubulins and actin, thus regulating the process of type 2 diabetes disease [8]. Moreover, some studies compared the proteome variations in the process of Jurkat cell apoptosis induced by *Aggregatibacter actinomycetemcomitans* cytolethal distending toxin and found that the expression of PTPLAD1 was downregulated, indicating that PTPLAD1 plays a role in the apoptosis of Jurkat cells [9]. Although the functional role of PTPLAD1 has been identified in several disease types, its role in cancers, especially colon cancer, remains unclear. In this study, we performed *in vitro* and *in vivo* experiments to determine the function of PTPLAD1 in cancer metastasis, as well as its clinical significance in colon cancer.

Signaling pathway disorder in cells is responsible for most carcinogenesis [10, 11]. The PHB-Raf-ERK signaling pathway was reported to be involved in cancer metastasis and is activated in most metastatic cancers [12, 13]. Briefly, prohibitin (PHB) located in plasma membrane lipid rafts interacts with C-Raf1 (Raf), and induces the activation of Raf and its downstream effectors such as ERK and Snail, thus finally inducing cell metastasis [12]. During this biological process, phosphorylation of PHB at Tyr259 (Y259) is necessary for PHB to activate Raf. A previous study reported that protein tyrosine phosphatase-like (PTPLA) shows the ability to dephosphorylate phosphotyrosine [14]. Here, our study demonstrated that the C-terminus or the PTPLA domain of PTPLAD1 interacts with PHB directly and dephosphorylates it at Y259. Interestingly, the middle peptide of PTPLAD1 is also necessary for the interaction between PHB and PTPLAD1. Dephosphorylation of PHB induced by PTPLAD1 results in the inactivation of Raf and downstream cascades, thus suppressing colon cancer metastasis.

Epigenetic modification regulates the expression of most genes [15]. and histone acetylation is one of the most common epigenetic modifications [16, 17]. Sodium butyrate is a histone deacetylase (HDAC) inhibitor that promotes the acetylation of histones, thus leading to the expression of certain genes [18, 19]. The *PTPLAD1* gene was first identified in sodium butyrate-treated cells [4] and a previous study reported that the transcription of the *PTPLAD1* gene was regulated by histone H4 acetylation in the promoter region [20]. However, our results demonstrated that histone H3K9 acetylation in the PTPLAD1 promoter region also shows a significant impact on PTPLAD1 transcription.

In the field of drug discovery, the concept of “old drugs for new applications” is gaining increasing recognition [21]. The identification of additional functions for a clinical drug would extend the scope of its clinical application. In this study, we validated the important role of the PHB-Raf-ERK signaling pathway in colon cancer metastasis and demonstrated that the interaction of PHB-Raf is necessary for the activation of Raf and downstream cascades. Therefore, we screened a drug library consisting of 440 Food and Drug Administration (FDA)-approved compounds, hoping to locate an “old drug” that has the potential to disrupt the PHB-Raf interaction and suppress colon cancer metastasis. Our results demonstrated that avobenzone, a dibenzoylmethane derivative, could significantly abrogate the PHB-Raf interaction.

Avobenzone is an oil-soluble ingredient that is traditionally used in sunscreen products to absorb the full spectrum of UVA rays [22]. A recent study illustrated that avobenzone suppresses the growth of human trophoblast cells and induces apoptosis by disrupting mitochondrial stability [23]. Another study verified that avobenzone could induce obesogenic phenotypes in normal human epidermal keratinocytes and mesenchymal stem cells [24]. For the first time, our study demonstrated that avobenzone could suppress colon cancer metastasis by blocking the PHB-Raf interaction, indicating that avobenzone may act as a promising targeted drug in metastatic colon cancer treatment.

Methods

Cell lines and drugs

Human colon cancer cells, SW480, SW620, HCT116, RKO, and FHs 74 Int (ATCC, Rockville, MD), were maintained in 1640 medium supplemented with 10% fetal bovine serum (Thermo Fisher Scientific, Waltham, MA, USA) at 37°C with 5% CO_2. The HCT116 highly invasive (HCT116 I8) cell line was screened by using repeated invasion assays as previously described [25]. All the cell lines were authenticated by short tandem repeat profiling and tested for mycoplasma contamination. U0126, trichostatin A (TSA) and avobenzone were purchased from Selleck Chemicals (Houston, TX, USA). Respectively, U0126 (10mM, 10mg in 2.34mL dimethyl sulfoxide (DMSO)), TSA (10mM, 5mg in 1.65mL DMSO), and avobenzone (10mM, 10mg in 3.22mL DMSO) were dissolved for in vitro usage. Avobenzone (2mg/mL, 14mg) was dissolved in corn oil (7mL) for in vivo usage.

Mass spectrometry and bioinformatics analyses

Cells were lysed by lysis buffer (Cell Signaling Technology, Danvers, MA, USA), and the cell lysates were further digested by trypsin (Hualishi Scientific, Beijing, China) through filter-aided sample preparation (FASP). The peptide samples were then dried by vacuum freeze and redissolved in trifluoroacetic acid (TFA) (0.5% in Water, Optima LC/MS Grade, Fisher Chemical) solution. After further desalination through MonoTIPTM C18 Pipette Tips (GL Sciences, Tokyo, Japan), the peptide samples were loaded and analyzed using an Orbitrap Fusion Lumos mass spectrometer (Thermo Fisher Scientific). Then, the raw data were analyzed through Spectronaut software (Omicsolution Co., Ltd., Shanghai, China), and the

differentially expressed proteins were analyzed by Ingenuity Pathway Analysis (IPA, Ingenuity Systems, Redwood City, CA, USA).

Plasmids, siRNAs and transfection

Flag-PTPLAD1 and Flag-PHB plasmids were generated by PCR amplification of sequences obtained from a colon cancer cDNA library and cloned into a pcDNA3.1 vector. The following primers were used to generate the PTPLAD1 and PHB plasmids: PTPLAD1: forward (5'-CGCGGATCCATGGAGAATCAGGTGTTGACGCCGC-3') and reverse (5'-CGCGAATTCTTACTTGTCATCGTCGTCCTTGTAGTCGTGGATCTTTTTCTTTTTTTGTC-3'); PHB: forward (5'- CGCGGATCCCATGGCTGCCAAAGTGTTT -3') and reverse (5'- CGCGAATTCTTACTTGTCATCGTCGTCCTTGTAGTCCTGGGGCAGCTGGAGGAGCACGGAC -3'). Transfections were performed using Lipofectamine^{TM} 3000 reagent (Thermo Fisher Scientific) according to the manufacturer's recommendations. HCT116 cells stably expressing PTPLAD1, PHB, and PTPLAD1+PHB or GFP control genes were established with approximately 2 weeks of puromycin selection as described previously [26]. The siRNA sequences and primers used to generate other plasmids are listed in Supplementary Tables S1 and S2.

Western blotting

The cell pellets were suspended in lysis buffer (Cell Signaling Technology, Danvers, MA, USA) and incubated on ice for 30 min. The cell lysates were subsequently centrifuged at 14000 g for 30 min at 4°C, after which supernatant was mixed with loading buffer and boiled for 10 min at 95°C before being loaded onto a sodium dodecyl sulfate (SDS) polyacrylamide gel for electrophoresis. The proteins were subsequently transferred to polyvinylidene fluoride (PVDF) membranes (Millipore, Billerica, MA, USA). After being blocked with 5% fat-free milk in Tris-buffered saline-Tween 20 (TBST), the membranes were probed with the appropriate primary antibodies, followed by the corresponding horseradish peroxidase (HRP)-conjugated secondary antibodies (Cell Signaling Technology). The signals were detected by Clarity Western ECL Substrate (Bio-Rad, Hercules, CA, USA) and visualized by exposure to autoradiographic film. Antibodies against the following proteins were used for the experiment: PHB (#60092-1-Ig), ERK (#66192-1-Ig) and Raf1 (#51140-1-AP) were obtained from Proteintech Group (Chicago, IL, USA); phospho-c-Raf (Ser338, #9427) was obtained from Cell Signaling Technology (Danvers, MA, USA); and phospho-ERK 1/2 (#ab50011) and PTPLAD1 (#ab139063) were obtained from Abcam (Cambridge, MA, USA).

Boyden Chamber Invasion Assay

Cell invasion assays were performed with an 8-μm pore size invasion chamber coated with 5% Matrigel (BD Biosciences, San Jose, CA, USA) in serum-free 1640 medium. Cells were suspended in serum-free medium and seeded into the upper chamber, and the lower compartment was filled with complete medium. After incubation at 37°C and 5% CO_2 for 36 h, the invaded cells adhering to the bottom surface of the chamber membrane were fixed with methanol and then stained with crystal violet (0.2% in

methanol). Images of three different fields were captured from each membrane, and the number of invaded cells was counted.

Quantitative real-time PCR (qRT-PCR)

qRT-PCR was performed as described previously [27]. In brief, total RNA was isolated using TRIzol reagent according to the manufacturer's protocol (Invitrogen). cDNA was synthesized using the PrimeScript™ II 1st Strand cDNA Synthesis Kit (Takara, Dalian, China). The mRNA expression levels of PTPLAD1 and the GAPDH control were detected by real-time PCR using SYBR® Premix Ex Taq™ II (Takara). The primers used were 5’-GCCTAAATAAACGCCGACT -3’ (forward) and 5’- AGAATCGCACAGTCAGGTT-3’ (reverse) for ANKRD1 and 5’-GAAGGTGAAGGTCGGAGTC-3’ (forward) and 5’-AAGATGGTGATGGGATTTC-3’ (reverse) for GAPDH.

Coimmunoprecipitation (Co-IP)

The cell lysates were prewashed with IgG (Santa Cruz Biotechnology) and protein A/G Sepharose beads (Invitrogen, Gaithersburg, MD) for 1 h at 4°C, and the cell supernatants were incubated with the appropriate primary antibody overnight at 4°C before being incubated with protein A/G Sepharose beads for 4 h. The beads were washed thrice with lysis buffer and eluted in 2 × SDS/PAGE loading buffer for immunoblotting. For LC-MS/MS analysis, the lanes on the silver-stained gels were cut into several bands and digested in an in-gel, after which the peptide mixtures were analyzed by LC-MS/MS.

Confocal assay

Cells were transiently co-transfected with PTPLAD1-mCherry and PHB-GFP plasmids for 48 h and then fixed in 4% paraformaldehyde. The cells were subsequently stained with 40,6-diamidino-2-phenylindole (DAPI, Thermo Fisher Scientific, Waltham, MA, USA) and observed by laser scanning confocal microscopy (Carl Zeiss AG, Jena, Germany).

Chromatin immunoprecipitation (ChIP) assay

The chromatin immunoprecipitation (ChIP) assay was performed by using the simple ChIP enzymatic chromatin IP kit (Cell Signaling, Beverly, MA, USA) according to the manufacturer's manual. Briefly, in vivo protein and DNA crosslinking was performed using 37% formaldehyde, followed by sonication and chromatin digestion. The protein–DNA complexes were immunoprecipitated by using the acetylated H3K9 antibody or negative control IgG antibody. After elution and reversal of crosslinking with proteinase K, the purified DNA was subjected to qRT-PCR analysis (Bio-Rad).

Experimental metastasis assay in mice

Female NCD mice aged 5-8 weeks were maintained under standard conditions and cared for according to the institutional guidelines for animal care. PTPLAD1 stably expressing or knocked down cells, as well as the corresponding negative control cells, were constructed based on ectopic luciferase expression in

HCT116 cells (i.e., PTPLAD1-overexpressing cells. HCT116-Luc). Approximately 1×10^6 HCT116 cells were suspended in phosphate buffered saline (PBS) and injected intravenously through the lateral tail vein of the mice. For pharmacological experiments, the animals were treated every three days with avobenzone (10 mg/kg) or vehicle through intragastric administration after injection of cancer cells. Metastatic activity was assessed by counting tumor nodes in main organs, such as the lung, liver and kidney. The animals were euthanized at the end of the experiment (21 days), and the main organs were collected for further analyses, such as histological analysis. All animal experiments were approved by the Ethics Committee for Animal Experiments of Jinan University.

Tissue samples

Fifteen pairs of colon tumor tissues and adjacent nontumor tissues were used for qRT-PCR and ChIP assays. Ethical consent was granted from the Ethical Committee Review Board of Jinan University.

Purification of Raf1-His and PHB-GST fusion proteins

Protein purification was performed as described previously [28]. The Raf gene was amplified with genomic DNA from HCT116 cells by PCR using the forward primer
5’- CGCGGATCCGCATCAATGGAGCACATACAGG -3’ and the reverse primer
5’- CGCGAATTCGAAGACAGGCAGCCTCGGGGAC -3’ and cloned into the pET-28b vector with a His tag. The PHB gene was amplified using the forward primer 5’- CGCGGATCCGAGGGTCCAGCAGAAGGAAAC -3’ and reverse primer 5’- CGCGAATTCGTGCAGGCAGGGTGGGCCCTCA -3’ and cloned into the pGEX-4T-1 vector with GST flag. Raf and PHB expression plasmids were transformed into E. coli BL21 star (DE3) cells for subsequent expression. The bacteria were grown to an optical density at 600 nm (OD600) of approximately 1.0 at 37°C, induced with 0.5 mM isopropyl β-D-thiogalactopyranoside (IPTG) for 6 h and lysed via sonication. Raf1-his and PHB-GST fusion proteins were isolated by loading whole cell lysate across His-binding and GST-binding columns according to the manufacturer’s instructions (Beyotime Biotechnology, Shanghai, China) and verified by SDS-PAGE and western blotting.

Enzyme-linked immunosorbent assay (ELISA) screening system

The experiment was performed as described previously [29]. Briefly, the first layer antibody His-tag antibody (Proteintech) in coating buffer (1 ng/μL) was added to a 96-well plate and cultured overnight at 4°C. After washing with PBS and blocking with 5% bovine serum albumin (BSA), the purified fusion protein Raf-His (1 μg) was added, and the plate was softly rocked for 5 h at room temperature. The plate was then incubated with 1 μg purified PHB-GST protein for 3 h at 37°C, and 440 small molecular inhibitors (10 μM) from the FDA-approved Drug Library (Selleck Chemicals, USA) were added individually into each well. After incubation with GST-tagged antibody, the corresponding secondary antibody and tetramethylbenzidine (TMB), the absorbance was measured at wavelengths of 450 nm and 630 nm. The level of Raf-PHB interaction was determined using the formula O.D.450-O.D.630. Coating buffer, TMB and termination buffer were purchased from NeoBioscience (Shenzhen, China).

Statistical analysis

The results were analyzed by using GraphPad PRISM software (GraphPad Software Inc., San Diego, CA, USA), and the data from different experiments were compared by Student's t-test and expressed as the mean ± SD. Sample size in animal experiments was chosen based on the literature documentation of similar well-characterized experiments, and no statistical method was used to predetermine sample size. Pearson's chi-square test was performed to analyze the association between PTPLAD1 expression levels and categorical clinicopathological variables. Survival analysis was performed using the Kaplan-Meier method with the log-rank test. $P < 0.05$ was considered statistically significant.

Results

PTPLAD1 is downregulated in highly invasive cancers and plays a role in suppressesing colon cancer cell metastasis *in vitro* and *in vivo*

To identify proteins related to metastasis in colon cancer cells, we firstly evaluated the invasion ability of serval colon cancer cell lines (**Figure 1A** and **Supplementary Figure S1**), and compared the differentially expressed proteins between SW480 and SW620 colon cancer cell lines with different invasion abilities obtained from one patient by using data-independent acquisition mass spectrometry (DIA-MS). Among the proteins identified, the expression of PTPLAD1 was significantly downregulated in SW620 cells, further verified by analyzing four cases of cancer metastasis-related mass spectrometry proteomics data accessible on the ProteomeXchange Consortium (dataset identifiers PXD016912, PXD015120, and PXD009744) (**Figure 1B**). To further clarify the correlation between PTPLAD1 and cancer cell metastasis, we detected the expression of PTPLAD1 in SW480/SW620 and HCT116/HCT116 I8, as well as the normal small intestine epithelial cells by using western blotting assay, the data showed that when compared with the low invasive cells, the expression of PTPLAD1 in highly invasive cells was significantly downregulated (**Figure 1C**). Moreover, a tissue PCR array also demonstrated that the expression of PTPLAD1 in tumor tissues was lower than in corresponding normal tissues (n = 15, **Figure 1D**). These data indicates that PTPLAD1 may participate in colon cancer metastasis.

In consideration of the significant correlation between PTPLAD1 expression and tumor malignancy, we then explored the role of PTPLAD1 in cancer cell metastasis. First, we transfected the colon cancer cell lines HCT116 and RKO with PTPLAD1-expressing plasmids, and the following Boyden chamber invasion assays showed that overexpression of PTPLAD1 suppressed cancer cell invasion (**Figure 1E**). In contrast, knockdown of PTPLAD1 promoted the invasion ability of cancer cells (**Figure 1F**). To further verify the tumor-suppressor role of PTPLAD1 in colon cancer, we detected the variation in several EMT markers in cells with different PTPLAD1 expression levels. The western blotting data in **Figure 1G** show that PTPLAD1 overexpression promoted the expression of epithelial cell markers such as E-cadherin and inhibited the expression of mesenchymal cell markers such as Fibronectin, Vimentin and Snail. Conversely, knockdown of PTPLAD1 prohibited epithelial cell marker expression and promoted

mesenchymal cell marker expression (**Figure 1H**). These results indicated that the expression of PTPLAD1 suppressed the EMT process of cancer cells.

We further identified the functional role of PTPLAD1 in colon cancer metastasis *in vivo*. HCT116 cell sublines stably expressing or knocking down PTPLAD1 were constructed and injected into NCD mice intravenously. Four weeks after the injection, the mice were euthanized, and the main organs, such as the lung, liver and kidney, were isolated for metastatic tumor node counting and pathological analysis. As shown in **Figure 1I**, overexpression of PTPLAD1 significantly suppressed the multiple organ metastasis of colon cancer cells, while knockdown of PTPLAD1 led to more serious metastasis (**Figure 1J**). Moreover, we collected the main organs of mice and evaluated the metastasis status by HE staining, data show that the overexpression of PTPLAD1 prohibited the metastasis of cancer cells to the lung, liver and kidney; instead, knockdown of PTPLAD1 promoted the metastasis of cancer cells to the organs mentioned (**Supplementary Figure S2**). Above all, our results demonstrated that PTPLAD1 is a tumor suppressor that takes part in suppressing colon cancer metastasis *in vitro* and *in vivo* by prohibiting the EMT process.

PTPLAD1 suppresses the activation of the Raf/ERK/Snail signaling pathway

To further clarify the role of PTPLAD1 in suppressing colon cancer metastasis, we subsequently performed a series of experiments. First, HCT116 cells were transiently transfected with PTPLAD1-flag-expressing plasmids for 36 hours. Co-IP assays were performed by using a flag-tagged antibody, and the immunoprecipitated proteins were identified by mass spectrometry analysis. In addition, HCT116 cells were transfected with PTPLAD1 interference RNA (si-PTPLAD1) for 24 hours, and then the whole proteins in cells were collected for mass spectral identification. Finally, both the immunoprecipitated and differentially expressed proteins were gathered for ingenuity pathway analysis (IPA analysis). As shown in **Figure 2A**, PTPLAD1 was significantly classified into Raf/ERK signaling cascades, indicating that PTPLAD1 played a role in the Raf/ERK/Snail signaling pathway. Then, we transiently transfected HCT116 and RKO colon cancer cells with PTPLAD1-expressing plasmids, and the expression of PTPLAD1, Raf, ERK and Snail, as well as the activation status of Raf and ERK, were detected by western blotting. The data shown in **Figure 2B** demonstrated that the activity of Raf and ERK, as well as the expression of Snail, was significantly inhibited by PTPLAD1 overexpression. In contrast, when PTPLAD1 expression was inhibited in colon cancer cells, the western blotting data showed the opposite effect (**Figure 2C**), indicating that the expression of PTPLAD1 suppressed the Raf/ERK/Snail signaling pathway. To further verify the role of PTPLAD1 in inactivating the ERK signaling pathway, we treated HCT116 and RKO cells with si-PTPLAD1 or the combined use of si-PTPLAD1 and U0126, a selective ERK inhibitor, for 24 hours. The following western blotting assays demonstrated that both the activation of ERK and the variation in EMT markers induced by PTPLAD1 knockdown could be abolished by U0126 treatment (**Figure 2D**). Likewise, the invasion of HCT116 and RKO cells induced by PTPLAD1 knockdown could also be abrogated by U0126 (**Figure 2E**). These data indicated that PTPLAD1 suppressed colon cancer cell invasion by abrogating the activation of the Raf/ERK/Snail signaling pathway.

PTPLAD1 interacts with PHB via the middle peptide and C-terminus

To explore the molecular mechanism of PTPLAD1 in suppressing colon cancer metastasis, we performed Co-IP assays in HCT116 cells transfected with PTPLAD1-expressing plasmids, and liquid chromatography-tandem mass spectrometry (LC-MS/MS) assays were performed to identify PTPLAD1-interacting proteins. Through bioinformatic analysis, 32 proteins that specifically interacted with PTPLAD1 were detected (**Figure 3A** and **Supplementary Table S3**). Among them, the PHB protein, which plays an important role in promoting carcinogenesis, attracted our attention [12]. We then performed Co-IP and confocal assays to confirm the LC-MS/MS analysis results. HCT116 cells were transfected with PTPLAD1- or PHB-expressing plasmids, Co-IP assays were performed by using a flag-tagged antibody, and the following western blotting assays confirmed the interaction between PTPLAD1 and PHB (**Figure 3B** and **3C**). To further demonstrate the interaction of PTPLAD1 and PHB, we co-transfected HCT116 cells with PHB-GFP- and PTPLAD1-mCherry-expressing plasmids and performed immunofluorescence assays. The following laser scanning confocal microscopy analysis demonstrated that PTPLAD1 and PHB were colocalized in colon cancer cells, indicating the interaction of PTPLAD1 and PHB (**Figure 3D**).

We next tried to determine which sections of PTPLAD1 bind to PHB directly. The structure of PTPLAD1 can be divided into three parts: the cs domain in the N-terminus, the PTPLA domain in the C-terminus, and the middle peptide between two domains. We thus constructed plasmids containing flag-tag fused with the cs domain (N), PTPLA domain (C), or middle peptides (M) and transfected them into HCT116 cells, and the following Co-IP assays were performed by using a flag-tag antibody to evaluate the binding affinity of different parts of PTPLAD1 to PHB. Unfortunately, the interaction with PHB was not detected in any of the three segments, indicating that the segments could not bind to PHB individually (**Supplementary Figure S3**). Then, we divided these three segments into different groups via pairwise combination to further identify the binding section of PTPLAD1 when interacting with PHB. Different plasmids containing flag-tag fused with N- and C-terminal (N/C), or N-terminal and M peptide (N/M), or M peptide and C-terminal (M/C), as well as the wild type PTPLAD1 were constructed and transfected into HCT116 cells, then Co-IP assays were performed by using a flag-tag antibody. The data shown in **Figure 3E** and **3F** demonstrated that the combination of M/C, rather than the other two combinations (N/C and N/M), could directly bind to PHB, indicating that the M peptide and C-terminal are important for the interaction of PTPLAD1 and PHB. Collectively, our results demonstrated that PTPLAD1 interacted with PHB in colon cancer cells and that the M peptide and PTPLA domain of PTPLAD1 were necessary for the interaction.

PTPLAD1 suppresses PHB/Raf/ERK/Snail signaling cascades by dephosphorylating PHB at Y259

Since our results indicate that PTPLAD1 interacts with PHB and suppresses colon cancer cell invasion by inhibiting Raf-ERK signaling cascades, we then explored the role of PHB in PTPLAD1-induced Raf-ERK signaling pathway inhibition. Previous studies demonstrated that PHB interacted with Raf to activate it and finally induced the activation of ERK [12, 30]; then, activated ERK promoted the transcription of many oncogenes, such as Snail [31]. Our data clarified that the PTPLA domain of PTPLAD1 was necessary for the interaction of PTPLAD1 and PHB, and previous studies identified that PTPLA plays an important role in tyrosine dephosphorylation [14, 32]. In addition, published papers reported that the phosphorylation of

PHB at Y259 was necessary for PHB interacting with and activating Raf [30]; thus, we performed several assays to identify whether PTPLAD1 inactivated the Raf-ERK signaling pathway by dephosphorylating PHB at Y259. HCT116 and RKO cells were transfected with a PTPLAD1-expressing plasmid, and the expression of PTPLAD1 and PHB, as well as the phosphorylation of PHB, were examined by western blotting. As shown in **Figure 4A**, overexpression of PTPLAD1 significantly suppressed the phosphorylation of PHB Y259, while knockdown of PTPLAD1 exerted the opposite effect (**Figure 4B**). Moreover, western blotting assays performed in colon cancer cells co-transfected with PTPLAD1- and PHB-expressing plasmids indicated that the inactivation of PHB/Raf/ERK/Snail signaling cascades induced by PTPLAD1 overexpression could be abrogated by PHB expression (**Figure 4C**), and the activation of the signaling pathway induced by knockdown of PTPLAD1 could also be abolished by knockdown of PHB (**Figure 4D**).

We then performed functional experiments to further verify whether PTPLAD1 suppressed tumor metastasis by inactivating PHB. HCT116 and RKO cells were co-transfected with PTPLAD1- and PHB-expressing plasmids, and the following Boyden chamber invasion assays indicated that the suppression of cell invasion induced by PTPLAD1 overexpression could be abolished by PHB overexpression (**Figure 4E**). In contrast, cell invasion induced by knockdown of PTPLAD1 could be prohibited by PHB knockdown (**Figure 4F**). In conclusion, PTPLAD1 suppresses the PHB/Raf/ERK/Snail signaling pathway by dephosphorylating PHB at Y259 and finally leads to the prohibition of colon cancer metastasis.

Histone H3K9 acetylation promotes PTPLAD1 transcription

To clarify the reason for the different expression levels of PTPLAD1 in tumor tissues and in normal tissues, we next performed a series of assays to explore the upstream regulation of PTPLAD1 in colon cancer cells. Previous studies reported that the transcription of the PTPLAD1 gene could be regulated by deacetylase inhibitors [20]. In this study, we treated HCT116 and RKO cells with trichostatin A (TSA), a selective HDAC inhibitor, and the following western blotting assays demonstrated that the acetylation of histone H3K9 was significantly enhanced (**Figure 5A**). Interestingly, qRT-PCR assays performed in TSA-treated colon cancer cells confirmed that the expression of PTPLAD1 was also upregulated (**Figure 5B**). To further explore the relationship of PTPLAD1 expression and histone H3K9 acetylation, we treated HCT116 and RKO cells with TSA and performed chromatin immunoprecipitation (ChIP) assays by using a histone H3K9 acetylation antibody, followed by the detection of the content of promotor DNA of PTPLAD1 by using qRT-PCR. The data in **Figure 5C** demonstrate that the PTPLAD1 promotor significantly accumulated at histone H3 when treated with TSA, indicating that the acetylation of H3K9 strengthened the interaction of the PTPLAD1 promotor and histone H3K9. Subsequently, ChIP assays were further performed in clinical tissues to identify the interaction of the PTPLAD1 promoter and histone H3 by using a histone H3K9 acetylation antibody, and qRT-PCR showed that the binding strength of H3K9 and the PTPLAD1 promoter in normal tissues was stronger than the binding strength of H3K9 and the PTPLAD1 promoter in tumor tissues (**Figure 5D**), which might explain why the expression of PTPLAD1 was lower in tumor tissues than in normal tissues. To further identify the correlation of PTPLAD1 transcription and H3K9 acetylation, we collected 15 pairs of clinical colon cancer tissues and corresponding normal tissues

to examine the transcription level of PTPLAD1 by qRT-PCR assays and the acetylation level of H3K9 by western blotting. Then, the correlation of PTPLAD1 expression and H3K9 acetylation was analyzed, and the data shown in **Figure 5E** demonstrated that a higher H3K9 acetylation level was always followed by a higher PTPLAD1 mRNA level, indicating a positive regulation of H3K9 acetylation on PTPLAD1 transcription. Collectively, our data validated that the expression of PTPLAD1 was promoted by H3K9 acetylation.

Avobenzone disrupts the PHB-Raf interaction and suppresses colon cancer metastasis

Our results demonstrated that PTPLAD1 suppresses colon cancer metastasis by prohibiting the activation of the PHB/Raf/ERK/Snail signaling pathway, and a previous study validated that the interaction of PHB and Raf is necessary for the activation of Raf and its downstream cascades [30]. Thus, we tried to screen out a small molecular drug targeting the PHB-Raf interaction. Raf-His and PHB-GST proteins were expressed and purified to construct a small molecule screening system based on ELISA (**Figure 6A**) [29]. Then, we screened the FDA-approved drug library by using the screening system and expected to find one or more drugs that could replace the role of PTPLAD1 to suppress the PHB/Raf/ERK signaling pathway by disrupting the interaction of Raf and PHB. Among the 440 screened drugs, avobenzone, once used for protecting skin from ultraviolet rays, showed a potent effect in decreasing the interaction between PHB and Raf (**Figure 6B** and **6C**) [22]. We further identified the effect of avobenzone in disrupting the PHB-Raf interaction. HCT116 cells were treated with avobenzone, Co-IP assays were performed by using a PHB antibody, and western blotting assays demonstrated that avobenzone significantly disrupted the interaction of PHB and Raf (**Figure 6D**). In addition, western blotting assays performed in avobenzone-treated HCT116 cells showed that the activation of both Raf and MEK, a downstream effector of Raf, was significantly suppressed, indicating that the activation of Raf induced by the PHB-Raf interaction could be prohibited by avobenzone (**Figure 6E**). Functionally, HCT116 and RKO cells were treated with avobenzone, and the following western blotting and Boyden chamber invasion assays showed that the EMT process of the cells was prohibited and the invasion of colon cancer cells was also suppressed (**Figure 6F and 6G**). We further identified the inhibitory effect of avobenzone on colon cancer metastasis *in vivo*. A colon cancer metastasis mouse model was established by injecting HCT116-Luc cells into mice intravenously and then treating the mice with vehicle or avobenzone by intragastric administration. As shown in **Figure 6H**, compared with the vehicle group, mice treated with avobenzone showed a weaker metastasis level of cancer cells in the main organs, such as the lung, liver and kidney. We also evaluated the toxicity effect of avobenzone in organisms by using pathological analysis. Main organs such as lung, liver, and kidney were collected from the above vehicle- or avobenzone-treated mice, and the tissue morphological variations were examined by hematoxylin-eosin (H&E) staining. The data in **Figure 6I** show that avobenzone had no side effects in the main organs. Taken together, we screened out a small molecular drug termed avobenzone and confirmed that avobenzone suppressed colon cancer metastasis *in vitro* and *in vivo* by disrupting the interaction of PHB and Raf.

Discussion

Tumorigenesis is mostly induced by the activation of oncogenes or inactivation of tumor suppressor genes; therefore, it is necessary to explore novel genes or proteins involved in the progression of tumorigenesis to better understand cancer. Tumor metastasis induces poor prognosis and low overall survival, while the molecular mechanisms underlying metastasis remain complex and unclear. In this study, we compared the differences in proteomics between SW480 and SW620, two colon cancer cell lines derived from the same patient at different clinical stages. Among the proteins identified, we observed that the expression level of PTPLAD1 was significantly downregulated in SW620 cells, the highly invasive cell line, signifying that PTPLAD1 is a tumor suppressor in colon cancer cells. Previous studies claimed that PTPLAD1 promotes long-chain fatty acid synthesis and cell apoptosis, while the role of PTPLAD1 in cancer metastasis remains unknown. With a series of experiments performed *in vitro* and *in vivo*, we demonstrated that PTPLAD1 is involved in tumorigenesis and suppresses colon cancer metastasis by interrupting the Raf-ERK signaling pathway.

PHB protein is one of the Raf activator proteins that induces diverse biological processes in cancer, such as proliferation, differentiation and invasion [33, 34]. Activation of Raf induced by PHB results in the activation and nuclear translocation of ERK, a protein kinase that promotes the expression of many oncogenes, such as Snail [35, 36]. Previous studies reported that Y259 phosphorylation is necessary for PHB to activate Raf and downstream signaling pathways [12]. Our results identified that PTPLAD1 interacts with PHB directly and that the PTPLAD1 C-terminus is crucial for the interaction. Further studies demonstrated that PTPLAD1 dephosphorylates PHB at Y259, which results in the inactivation of PHB and Raf and downstream signals, thus inducing the suppression of colon cancer metastasis.

Epigenetic regulation, including histone acetylation, widely exists in tumorigenesis. Histone acetylation decreases the binding of histones and gene promoters, thus promoting gene transcription and increasing gene expression levels. A previous study demonstrated that the *PTPLAD1* gene promoter is regulated by histone deacetylase inhibitors by using an exogenous expression system, and the acetylation of histone H4 is crucial for the expression of the *PTPLAD1* gene [20]. In this study, we identified a positive correlation between H3 acetylation levels and *PTPLAD1* expression levels for the first time. Moreover, we compared 15 pairs of clinical samples and found that the H3K9 acetylation levels in tumor tissues were lower than the H3K9 acetylation levels in normal tissues, and *PTPLAD1* mRNA levels showed the same tendency. That is, *PTPLAD1* gene transcription is promoted by H3K9 acetylation.

The data of PTPLAD1 involved in tumorigenesis demonstrated the significance of the PHB-Raf-ERK signaling pathway in colon cancer metastasis, and the PHB-Raf interaction is a prerequisite for downstream signal activation. We thus performed a series of experiments to screen a small molecular inhibitor library targeting the PHB-Raf interaction. Finally, we found that avobenzone, a small molecule once used to protect skin from ultraviolet light, could interrupt the interaction of PHB and Raf. Further studies demonstrated that avobenzone prohibits the activation of the Raf-ERK signaling pathway and suppresses colon cancer invasion. Since we identified the function of avobenzone in suppressing colon

cancer metastasis, our next step was to uncover the specific mechanism by which avobenzone inhibited the PHB-Raf interaction, thus extending its usefulness in cancer therapy (Fig. 7).

Studies aiming to develop effective diagnostic and prognostic biomarkers for cancer are urgently needed. In this study, we found that PTPLAD1 plays an important role in tumor metastasis regulation in colon cancer and reported for the first time that PTPLAD1 is frequently downregulated in colon cancer. Our findings strongly suggested that PTPLAD1 may be a useful diagnostic biomarker for colon cancer. Colon cancer is the third most common malignant disease in men and the second most common malignant disease in women, and morbidity is rising among adolescents and young adults [37, 38]. Although Our study demonstrated the prognostic value of PTPLAD1 in colon cancer, the potential of PTPLAD1 as a prognostic marker in cancer warrants further investigation.

Conclusions

Our study highlighted the pivotal role of PTPLAD1 in suppressing colon cancer metastasis. PTPLAD1 performs its function through interacting with PHB and dephosphorylating it at Tyr259 and thus prohibits the activation of PHB and the downstream Raf/ERK/Snail signaling pathway. Based on the mode of action of PTPLAD1, we screened out a small molecular drug termed avobenzone from the FDA-approved drug library, which exhibits a potent effect in suppressing colon cancer cell metastasis. All in all, our study not only identifies a diagnostic useful biomarker, but also provides a potential targeted drug for metastatic colon cancer therapy.

Abbreviations

PTPLAD1, protein tyrosine phosphatase-like A domain containing 1; Co-IP, Co-immunoprecipitation; ChIP, Chromatin-immunoprecipitation; ELISA, Enzyme-linked immuno sorbent assay; PHB, prohibitin; Raf, C-Raf1; ERK, extracellular signal-regulated kinase; VLCFA, very long-chain fatty acid; HCV, hepatitis C virus; PTPLA, protein tyrosine phosphatase-like; HDAC, histone deacetylase; FDA, Food and Drug Administration; TSA, trichostatin A; DMSO, dimethyl sulfoxide; qRT-PCR, Quantitative real-time PCR; DIA-MS, data-independent acquisition mass spectrometry ; LC-MS/MS, liquid chromatography-tandem mass spectrometry.

Declarations

Ethics approval and consent to participate

Ethical consent was granted from the Ethical Committee Review Board of Jinan University. All animal experiments were approved by the Ethics Committee for Animal Experiments of Jinan University.

Consent for publication

Not applicable.

Availability of data and materials

All data generated or analyzed during this study are included in this published article and its supplementary information files.

Competing interests

The authors declare that they have no competing interests.

Funding

This work was supported by the National Key R&D Program of China (2017YFA0505100), the National Natural Science Foundation of China (82002466, 31770888, 31570828, 81672953, 81773085), and the China Postdoctoral Science Foundation (2020M673007, 2021T140765).

Authors' contributions

J. Y. and Y-J. L. performed the experiments, prepared the figures and wrote the manuscript; Y. H., W-X. Z., X. Y., J-Z. L., and X-H. H. took part in the mass spectrum analysis and data statistics; B. L. and Q-Y. H. designed the work, wrote and revised the manuscript.

Acknowledgements

Not applicable.

References

1. G. Lech, R. Slotwinski, M. Slodkowski, I.W. Krasnodebski, Colorectal cancer tumour markers and biomarkers: Recent therapeutic advances, World J Gastroenterol, 22 (2016) 1745-1755.
2. H. Cao, E. Xu, H. Liu, L. Wan, M. Lai, Epithelial-mesenchymal transition in colorectal cancer metastasis: A system review, Pathol Res Pract, 211 (2015) 557-569.
3. V. Hanusova, L. Skalova, V. Kralova, P. Matouskova, The Effect of Flubendazole on Adhesion and Migration in SW480 and SW620 Colon Cancer Cells, Anticancer Agents Med Chem, 18 (2018) 837-846.
4. D. Courilleau, E. Chastre, M. Sabbah, G. Redeuilh, A. Atfi, J. Mester, B-ind1, a novel mediator of Rac1 signaling cloned from sodium butyrate-treated fibroblasts, J Biol Chem, 275 (2000) 17344-17348.
5. M. Ikeda, Y. Kanao, M. Yamanaka, H. Sakuraba, Y. Mizutani, Y. Igarashi, A. Kihara, Characterization of four mammalian 3-hydroxyacyl-CoA dehydratases involved in very long-chain fatty acid synthesis, FEBS Lett, 582 (2008) 2435-2440.
6. S. Taguwa, T. Okamoto, T. Abe, Y. Mori, T. Suzuki, K. Moriishi, Y. Matsuura, Human butyrate-induced transcript 1 interacts with hepatitis C virus NS5A and regulates viral replication, J Virol, 82 (2008) 2631-2641.

7. S. Taguwa, H. Kambara, H. Omori, H. Tani, T. Abe, Y. Mori, T. Suzuki, T. Yoshimori, K. Moriishi, Y. Matsuura, Cochaperone activity of human butyrate-induced transcript 1 facilitates hepatitis C virus replication through an Hsp90-dependent pathway, J Virol, 83 (2009) 10427-10436.
8. M. Boutchueng-Djidjou, P. Belleau, N. Bilodeau, S. Fortier, S. Bourassa, A. Droit, S. Elowe, R.L. Faure, A type 2 diabetes disease module with a high collective influence for Cdk2 and PTPLAD1 is localized in endosomes, PLoS One, 13 (2018) e0205180.
9. H.P. Chen, L. Li, X. Chen, M.F. Yang, Y. Ye, X.Q. Wang, Y. Xu, The mechanism of Jurkat cells apoptosis induced by Aggregatibacter actinomycetemcomitans cytolethal distending toxin, Apoptosis, 22 (2017) 841-851.
10. G. Courtois, T.D. Gilmore, Mutations in the NF-kappaB signaling pathway: implications for human disease, Oncogene, 25 (2006) 6831-6843.
11. D.A. Altomare, J.R. Testa, Perturbations of the AKT signaling pathway in human cancer, Oncogene, 24 (2005) 7455-7464.
12. J. Yang, B. Li, Q.Y. He, Significance of prohibitin domain family in tumorigenesis and its implication in cancer diagnosis and treatment, Cell Death Dis, 9 (2018) 580.
13. Z. Luan, Y. He, M. Alattar, Z. Chen, F. He, Targeting the prohibitin scaffold-CRAF kinase interaction in RAS-ERK-driven pancreatic ductal adenocarcinoma, Mol Cancer, 13 (2014) 38.
14. D.A. Uwanogho, Z. Hardcastle, P. Balogh, G. Mirza, K.L. Thornburg, J. Ragoussis, P.T. Sharpe, Molecular cloning, chromosomal mapping, and developmental expression of a novel protein tyrosine phosphatase-like gene, Genomics, 62 (1999) 406-416.
15. E. Porcellini, N. Laprovitera, M. Riefolo, M. Ravaioli, I. Garajova, M. Ferracin, Epigenetic and epitranscriptomic changes in colorectal cancer: Diagnostic, prognostic, and treatment implications, Cancer Lett, 419 (2018) 84-95.
16. C.Y. Yen, H.W. Huang, C.W. Shu, M.F. Hou, S.S. Yuan, H.R. Wang, Y.T. Chang, A.A. Farooqi, J.Y. Tang, H.W. Chang, DNA methylation, histone acetylation and methylation of epigenetic modifications as a therapeutic approach for cancers, Cancer Lett, 373 (2016) 185-192.
17. B.R. Selvi, S. Chatterjee, R. Modak, M. Eswaramoorthy, T.K. Kundu, Histone acetylation as a therapeutic target, Subcell Biochem, 61 (2013) 567-596.
18. M.C. Chang, Y.J. Chen, Y.C. Lian, B.E. Chang, C.C. Huang, W.L. Huang, Y.H. Pan, J.H. Jeng, Butyrate Stimulates Histone H3 Acetylation, 8-Isoprostane Production, RANKL Expression, and Regulated Osteoprotegerin Expression/Secretion in MG-63 Osteoblastic Cells, Int J Mol Sci, 19 (2018).
19. E. Contreras-Leal, A. Hernandez-Oliveras, L. Flores-Peredo, A. Zarain-Herzberg, J. Santiago-Garcia, Histone deacetylase inhibitors promote the expression of ATP2A3 gene in breast cancer cell lines, Mol Carcinog, 55 (2016) 1477-1485.
20. M. Sabbah, C. Saucier, G. Redeuilh, Human B-ind1 gene promoter: cloning and regulation by histone deacetylase inhibitors, Gene, 374 (2006) 128-133.
21. Q. Liu, Editorial: Old Drugs Learn New Tricks: Advances and Applications for Drug Repurposing, Curr Top Med Chem, 16 (2016) 3627-3628.

22. P. Kumar, A. Deshpande, Patent review on photostability enhancement of avobenzone and its formulations, Recent Pat Drug Deliv Formul, 9 (2015) 121-128.
23. C. Yang, W. Lim, F.W. Bazer, G. Song, Avobenzone suppresses proliferative activity of human trophoblast cells and induces apoptosis mediated by mitochondrial disruption, Reprod Toxicol, 81 (2018) 50-57.
24. S. Ahn, S. An, M. Lee, E. Lee, J.J. Pyo, J.H. Kim, M.W. Ki, S.H. Jin, J. Ha, M. Noh, A long-wave UVA filter avobenzone induces obesogenic phenotypes in normal human epidermal keratinocytes and mesenchymal stem cells, Arch Toxicol, (2019).
25. H.F. Hu, W.W. Xu, Y. Wang, C.C. Zheng, W.X. Zhang, B. Li, Q.Y. He, Comparative Proteomics Analysis Identifies Cdc42-Cdc42BPA Signaling as Prognostic Biomarker and Therapeutic Target for Colon Cancer Invasion, J Proteome Res, 17 (2018) 265-275.
26. W.W. Xu, B. Li, X.Y. Guan, S.K. Chung, Y. Wang, Y.L. Yip, S.Y. Law, K.T. Chan, N.P. Lee, K.W. Chan, L.Y. Xu, E.M. Li, S.W. Tsao, Q.Y. He, A.L. Cheung, Cancer cell-secreted IGF2 instigates fibroblasts and bone marrow-derived vascular progenitor cells to promote cancer progression, Nat Commun, 8 (2017) 14399.
27. B. Li, P. Hong, C.C. Zheng, W. Dai, W.Y. Chen, Q.S. Yang, L. Han, S.W. Tsao, K.T. Chan, N.P.Y. Lee, S. Law, L.Y. Xu, E.M. Li, K.W. Chan, Y.R. Qin, X.Y. Guan, M.L. Lung, Q.Y. He, W.W. Xu, A.L. Cheung, Identification of miR-29c and its Target FBXO31 as a Key Regulatory Mechanism in Esophageal Cancer Chemoresistance: Functional Validation and Clinical Significance, Theranostics, 9 (2019) 1599-1613.
28. K. Cao, N. Li, H. Wang, X. Cao, J. He, B. Zhang, Q.Y. He, G. Zhang, X. Sun, Two zinc-binding domains in the transporter AdcA from Streptococcus pyogenes facilitate high-affinity binding and fast transport of zinc, J Biol Chem, 293 (2018) 6075-6089.
29. J. Yang, W.W. Xu, P. Hong, F. Ye, X.H. Huang, H.F. Hu, Q.H. Zhang, X. Yan, B. Li, Q.Y. He, Adefovir dipivoxil sensitizes colon cancer cells to vemurafenib by disrupting the KCTD12-CDK1 interaction, Cancer Lett, 451 (2019) 79-91.
30. C.F. Chiu, M.Y. Ho, J.M. Peng, S.W. Hung, W.H. Lee, C.M. Liang, S.M. Liang, Raf activation by Ras and promotion of cellular metastasis require phosphorylation of prohibitin in the raft domain of the plasma membrane, Oncogene, 32 (2013) 777-787.
31. S.J. Lee, S.S. Park, Y.H. Cho, K. Park, E.J. Kim, K.H. Jung, S.K. Kim, W.J. Kim, S.K. Moon, Activation of matrix metalloproteinase-9 by TNF-alpha in human urinary bladder cancer HT1376 cells: the role of MAP kinase signaling pathways, Oncol Rep, 19 (2008) 1007-1013.
32. X. Lin, X. Yang, Q. Li, Y. Ma, S. Cui, D. He, X. Lin, R.J. Schwartz, J. Chang, Protein tyrosine phosphatase-like A regulates myoblast proliferation and differentiation through MyoG and the cell cycling signaling pathway, Mol Cell Biol, 32 (2012) 297-308.
33. A.L. Theiss, S.V. Sitaraman, The role and therapeutic potential of prohibitin in disease, Biochim Biophys Acta, 1813 (2011) 1137-1143.

34. A.S. Kathiria, W.L. Neumann, J. Rhees, E. Hotchkiss, Y. Cheng, R.M. Genta, S.J. Meltzer, R.F. Souza, A.L. Theiss, Prohibitin attenuates colitis-associated tumorigenesis in mice by modulating p53 and STAT3 apoptotic responses, Cancer Res, 72 (2012) 5778-5789.
35. B.N. Smith, L.J. Burton, V. Henderson, D.D. Randle, D.J. Morton, B.A. Smith, L. Taliaferro-Smith, P. Nagappan, C. Yates, M. Zayzafoon, L.W. Chung, V.A. Odero-Marah, Snail promotes epithelial mesenchymal transition in breast cancer cells in part via activation of nuclear ERK2, PLoS One, 9 (2014) e104987.
36. J. Zhao, B. Ou, D. Han, P. Wang, Y. Zong, C. Zhu, D. Liu, M. Zheng, J. Sun, H. Feng, A. Lu, Tumor-derived CXCL5 promotes human colorectal cancer metastasis through activation of the ERK/Elk-1/Snail and AKT/GSK3beta/beta-catenin pathways, Mol Cancer, 16 (2017) 70.
37. H. Brody, Colorectal cancer, Nature, 521 (2015) S1.
38. B.A. Weinberg, J.L. Marshall, M.E. Salem, The Growing Challenge of Young Adults With Colorectal Cancer, Oncology (Williston Park), 31 (2017) 381-389.

Figures

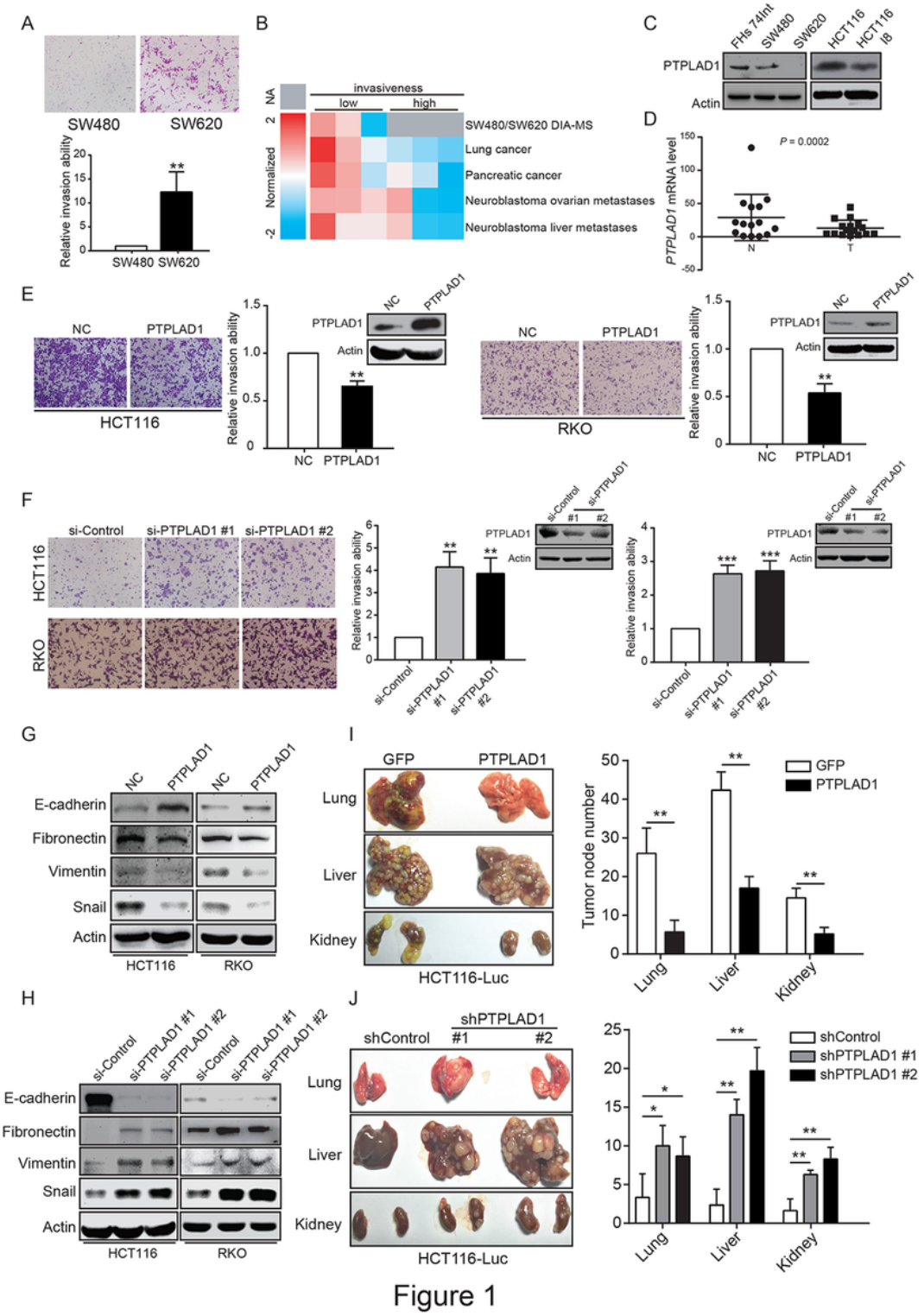

Figure 1

Figure 1

PTPLAD1 is downregulated in cancers and plays a role in suppressing colon cancer metastasis. A, Comparison of the invasive abilities of different colon cancer cell lines. Upper, pictures of cell invasion; Lower, statistics of the invaded cells. B, DIA-MS identified the expression of PTPLAD1 in SW620 and SW480 cells and in the other four cases of metastasis cancer-related mass spectrometry proteomics data accessible on the ProteomeXchange Consortium (PXD016912, PXD015120, PXD009744). C, The

expression of PTPLAD1 in SW480, SW620, HCT116, HCT116 I8 colon cancer cells and in FHs 47Int normal small intestine epithelial cells was examined by western blotting assays. D, The PTPLAD1 gene expression in tumor tissues and corresponding normal tissues was evaluated by qRT-PCR. 15 pairs of tissues were collected and analyzed. Bars, s.d.; *p < 0.05, ** p < 0.01 compared with the low invasive cancer cell. E-F, HCT116 and RKO cells were transfected with PTPLAD1-expressing plasmids (E) or a siRNA against PTPLAD1 (100 nM) (F), as well as the corresponding control vector and si-Control. The expression of PTPLAD1 was determined by western blotting, and the invasion ability of these cells was evaluated by Boyden chamber invasion assays. G-H, The expression of EMT markers in HCT116 and RKO cells transfected with PTPLAD1-expressing plasmids (G) or siRNAs (H) was determined by western blotting. I-J, HCT116-Luc cells with stable PTPLAD1 expression (I) or PTPLAD1 knockdown (J), as well as the corresponding control cells, were injected into mice intravenously, and the lung, liver and kidney were isolated to count the metastatic tumor nodes. Left, pictures of organs; right, statistics of tumor nodes in organs; 5 mice were used in each experimental group. In vitro data are presented of three independent experiments; Bars, s.d.; *p < 0.05, ** p < 0.01 compared with the control group.

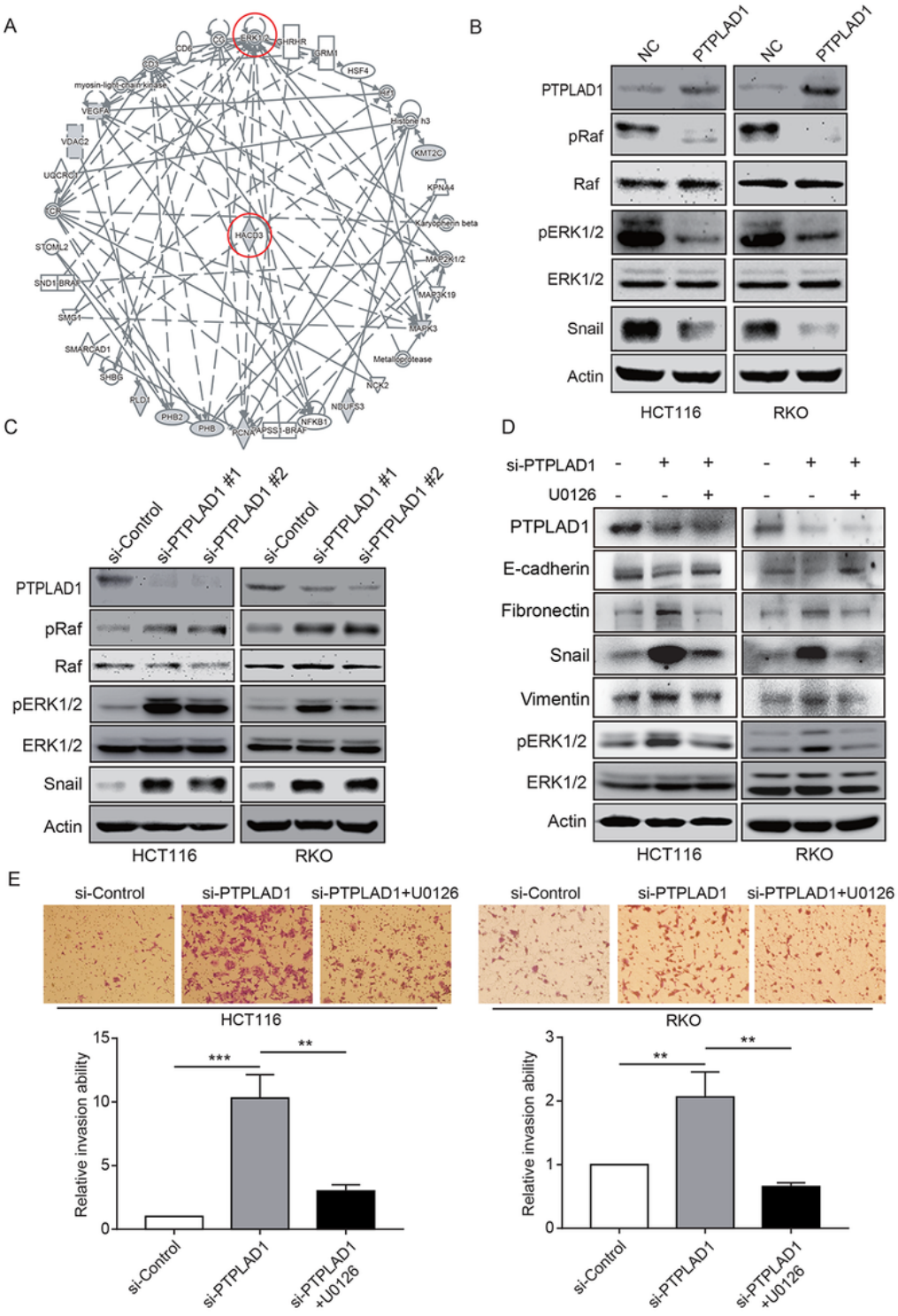

Figure 2

Figure 2

PTPLAD1 suppresses the activation of Raf-ERK signaling cascades. A, HCT116 cells were transfected with PTPLAD1-flag plasmids, and Co-IP assays were performed by using a flag antibody. The precipitated proteins were determined by LC-MS/MS and analyzed by IPA. Some proteins were enriched in the Raf-ERK signaling pathway. B-C, HCT116 and RKO cells were transfected with PTPLAD1-flag plasmids (B) or siRNAs against PTPLAD1 (C) and the corresponding controls. The expression of PTPLAD1, Raf, ERK1/2

and Snail, as well as the activation status of Raf (pRaf) and ERK1/2 (pERK1/2), were determined by western blotting. D-E, HCT116 and RKO cells were transfected with a siRNA against PTPLAD1 with or without the presence of the ERK1/2 inhibitor U0126, the activation status of ERK1/2 was detected by western blotting (D), and the invasion ability of HCT116 and RKO cells was evaluated by Boyden chamber invasion assays (E). Histogram, statistics of invaded cells; Data are presented from three independent experiments; Bars, s.d.; ** $p < 0.01$, *** $p < 0.001$ compared with the control group.

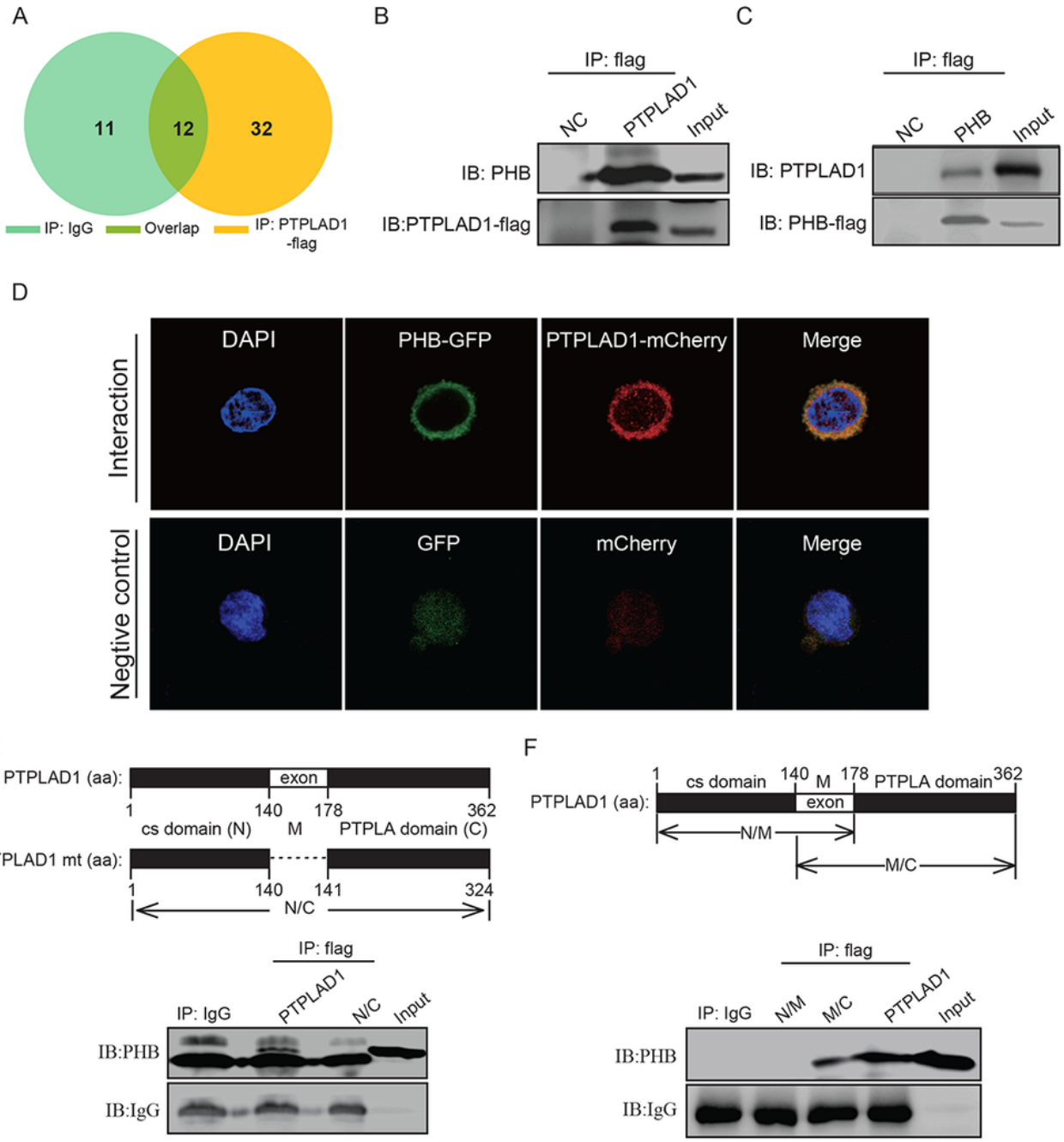

Figure 3

Figure 3

PTPLAD1 interacts with PHB through the middle peptide and C-terminus. A, HCT116 cells were transfected with PTPLAD1-flag plasmids and vector control, and whole cell lysates were immunoprecipitated with a flag antibody. Then, the immunoprecipitates were identified by using LC-MS/MS, and 32 proteins were detected in the immunoprecipitates. B-C, HCT116 cells were transfected with PTPLAD1-flag or PHB-flag plasmids, CoIP assays were performed by using a flag antibody, and the expression of PHB (B) and PTPLAD1 was detected by western blotting (C). D, HCT116 cells were co-transfected with PHB-GFP and PTPLAD1-mCherry plasmids, and confocal analysis of the localization of PTPLAD1 and PHB was performed in HCT116 cells. PHB, green; PTPLAD1, red; DAPI was used to stain the nuclei. E, HCT116 cells were transfected with PTPLAD1-flag or N/C-flag plasmids, Co-IP assays were performed by using a flag antibody, and the expression of PHB was detected by western blotting. Upper panel, structures of PTPLAD1 and N/M genes; IgG was considered the loading control. F, HCT116 cells were transfected with N/M, M/C or PTPLAD1-flag plasmids individually, Co-IP assays were performed by using a flag antibody, and the expression of PHB was determined by western blotting. Upper: structures of the N/M, M/C and PTPLAD1 genes; IgG was considered the loading control.

Supplementary Files

This is a list of supplementary files associated with this preprint. Click to download.

- Additionalfile2.pdf